



Stratospheric Response to Trace Gas Perturbations: Changes in Ozone and Temperature Distributions

Author(s): Guy Brasseur and Matthew H. Hitchman

Source: *Science*, New Series, Vol. 240, No. 4852 (Apr. 29, 1988), pp. 634-637

Published by: American Association for the Advancement of Science

Stable URL: <http://www.jstor.org/stable/1701373>

Accessed: 27-10-2017 18:53 UTC

REFERENCES

Linked references are available on JSTOR for this article:

http://www.jstor.org/stable/1701373?seq=1&cid=pdf-reference#references_tab_contents

You may need to log in to JSTOR to access the linked references.

JSTOR is a not-for-profit service that helps scholars, researchers, and students discover, use, and build upon a wide range of content in a trusted digital archive. We use information technology and tools to increase productivity and facilitate new forms of scholarship. For more information about JSTOR, please contact support@jstor.org.

Your use of the JSTOR archive indicates your acceptance of the Terms & Conditions of Use, available at <http://about.jstor.org/terms>



JSTOR

American Association for the Advancement of Science is collaborating with JSTOR to digitize, preserve and extend access to *Science*

14. R. Pool, *Science* **240**, 147 (1988).
15. We thank the following Du Pont colleagues for their assistance with this publication: P. M. Kelly, C. R. Walther, R. A. Oswald, W. J. Marshall, L. F.

Lardear, D. L. Smith, D. M. Groski, L. Cooke, C. M. Foris, A. J. Pawlowski, G. M. Hyatt, M. W. Sweeten, and N. Budynkiewicz.
30 March 1988; accepted 1 April 1988

Stratospheric Response to Trace Gas Perturbations: Changes in Ozone and Temperature Distributions

GUY BRASSEUR AND MATTHEW H. HITCHMAN

The stratospheric concentration of trace gases released in the atmosphere as a result of human activities is increasing at a rate of 5 to 8 percent per year in the case of the chlorofluorocarbons (CFCs), 1 percent per year in the case of methane (CH₄), and 0.25 percent per year in the case of nitrous oxide (N₂O). The amount of carbon dioxide (CO₂) is expected to double before the end of the 21st century. Even if the production of the CFCs remains limited according to the protocol for the protection of the ozone layer signed in September 1987 in Montreal, the abundance of active chlorine (2 parts per billion by volume in the early 1980s) is expected to reach 6 to 7 parts per billion by volume by 2050. The impact of these increases on stratospheric temperature and ozone was investigated with a two-dimensional numerical model. The model includes interactive radiation, wave and mean flow dynamics, and 40 trace species. An increase in CFCs caused ozone depletion in the model, with the largest losses near the stratopause and, in the vertical mean, at high latitudes. Increased CO₂ caused ozone amounts to increase through cooling, with the largest increases again near 45 kilometers and at high latitudes. This CO₂-induced poleward increase reduced the CFC-induced poleward decrease. Poleward and downward ozone transport played a major role in determining the latitudinal variation in column ozone changes.

HUMAN ACTIVITY HAS CAUSED A marked increase in the concentration of certain important trace gases in the atmosphere. These gases can have a significant impact on ozone, either directly through photochemistry or indirectly by changing the radiative budget and hence the temperature and chemistry (1). If the temperature structure changes, transport of chemicals by the mean circulation and waves can change. Ozone absorbs ultraviolet (UV) insolation, accounting for the basic structure of the stratosphere, in which temperature increases with altitude from the tropopause near 15 km to the stratopause near 50 km, and shields the biosphere from potentially harmful effects. It is of considerable interest to estimate the distribution in latitude and altitude of ozone and temperature changes due to increased trace gases.

Two-dimensional models (2-D; latitude and altitude) represent transport in a more realistic way than 1-D models, which provide globally averaged vertical distributions (2). Most of the previous perturbation studies performed with 2-D models indicated that the expected ozone depletion due to chlorofluorocarbons (CFCs) should be two to three times larger in the polar regions than in the tropics, with the strongest latitudinal gradient in depletion occurring in spring (3, 4). Other studies (5, 6) showed that increases in CO₂ can enhance ozone

amounts, with the largest increases near the pole. The recent study (6) raised the possibility that CFC-induced reductions might be reversed by larger CO₂-induced increases at high latitudes. The magnitude and sign of changes in the ozone column (number of ozone molecules above an area at the earth's surface) is governed primarily by changes in the lower stratosphere where most of the ozone resides. In this altitude range, chemistry, dynamics, and radiation play equally important roles, so that these processes and their interactions need to be represented as accurately as possible. The purpose of the present study is to assess, as a function of latitude and altitude, the response of the middle atmosphere to specified anthropogenic perturbations.

Ozone (O₃) is destroyed by chemical recombination with atomic oxygen, a process that is catalyzed by the presence of radicals such as OH, NO, ClO, and BrO (1). When CFCs reach the stratosphere they can be photodissociated, with the added chlorine catalytically destroying ozone. The temperature dependence of reactions involving ozone is such that ozone amounts will increase if temperatures decrease. Ozone and temperature are observed to be negatively correlated in the upper stratosphere (7). CO₂ efficiently emits infrared radiation to the earth and to space. In the middle atmosphere (tropopause to mesopause, ~80 km),

CO₂ increases would lead to more radiation to space and decreased temperatures. Thus CO₂ increases should lead to ozone increases. The latitudinal variation in predicted ozone changes has both photochemical and dynamical contributions. In the sunlight above 25 km, photochemistry plays a major role, whereas below 25 km and in the polar night, dynamical transport is relatively more important (4).

The 2-D model used in the present study extends from pole to pole with a latitudinal resolution of 5° and from the surface to 85 km with a vertical resolution of 1 km. The transformed Eulerian mean equations are used (8). This allows for a straightforward interpretation of the influence of waves. Absorption of gravity waves (9) and Rossby waves (10) drives the meridional circulation and mixes constituents in altitude and latitude, respectively. Calculated wave driving and eddy mixing coefficients vary with the evolving model zonal mean wind distribution. Wave driving, mixing coefficients, and temperature are specified below 15 km. Above 15 km, temperature evolves along with changes in the wave-driven circulation and changes in diabatic heating and is calculated with the evolving model fields of ozone and water vapor. The detailed radiative code is similar to the algorithm used in the latest version of the NCAR Community Climate Model (11). Included in the radiative calculation are absorption of UV insolation by O₃ and H₂O, near-infrared insolation by O₂ and H₂O, and absorption and emission of infrared radiation by CO₂, O₃, and H₂O. The distributions of chemical species are obtained by integrating their continuity equations, which are expressed in terms of the transformed Eulerian circulation. To avoid numerical problems associated with the broad spectrum of chemical lifetimes involved, the shortest lived species are grouped into quasi-conservative families (12). The adopted reaction rate constants, solar irradiance, and absorption cross sections were taken from recent compilations (13).

Figure 1 shows the changes in temperature and ozone as a function of latitude and height resulting from (i) a doubling of the CO₂ abundance from the current 350 parts per million by volume (ppmv) (run 1); (ii) increasing the mixing ratio of odd chlorine (Cl_x) in the upper stratosphere from 2.0 to 6.6 parts per billion by volume (ppbv) (run 2); and (iii) a combined scenario (run 3). The model does not include detailed physical parameterizations in the troposphere.

G. Brasseur, Belgian Institute for Space Aeronomy, 1180 Brussels, Belgium.
M. H. Hitchman, National Center for Atmospheric Research, Boulder, CO 80307.

For runs 1 and 3, surface and tropospheric air temperatures have been increased by an amount that varies linearly from 2 K at the equator to 4 K at the pole to account for the CO₂ greenhouse effect (14). Results are shown for the solstitial month of June, after 1 year of model integration (allowing for seasonal cycling).

Temperatures throughout the stratosphere and lower mesosphere are expected to cool from a doubling of CO₂ (Fig. 1A), with decreases of 8 to 15 K near the stratopause. Decreases tended to be larger at high latitudes. Decreases may be expected to be larger where the temperature is higher because of the strong temperature dependence

of the Planck function, and where the vertical curvature of temperature, hence layer to layer exchange, is strongest (15). The net effect is to diminish the sharpness of the stratopause and thereby reduce the vertical stability of the stratosphere and increase the stability of the mesosphere, and to also increase westerly winds in mid-latitudes due to stronger cooling at the poles. At high latitudes in the layer from 20 to 25 km, which contributes a large fraction of the column ozone abundance, the calculated cooling is 2 to 5 K. In this region these values are similar to those in (5), but are significantly smaller than the cooling of 8 to 10 K predicted by (6).

With lowered temperatures, ozone concentrations are enhanced (Fig. 1B), since its loss rate is slower at lower temperatures. Reductions in OH density (6) may also contribute. In the upper stratosphere an ozone increase of 20 to 30% is predicted where these mechanisms contribute significantly. Below 25 km and equatorward of 50°, ozone density is predicted to decrease. Here the "self-healing" effect dominates, in which increases in ozone at high altitudes result in decreased penetration of UV insolation to lower levels and a consequent decrease of ozone at lower levels. Thus the total column is somewhat resilient to vertically local changes in ozone.

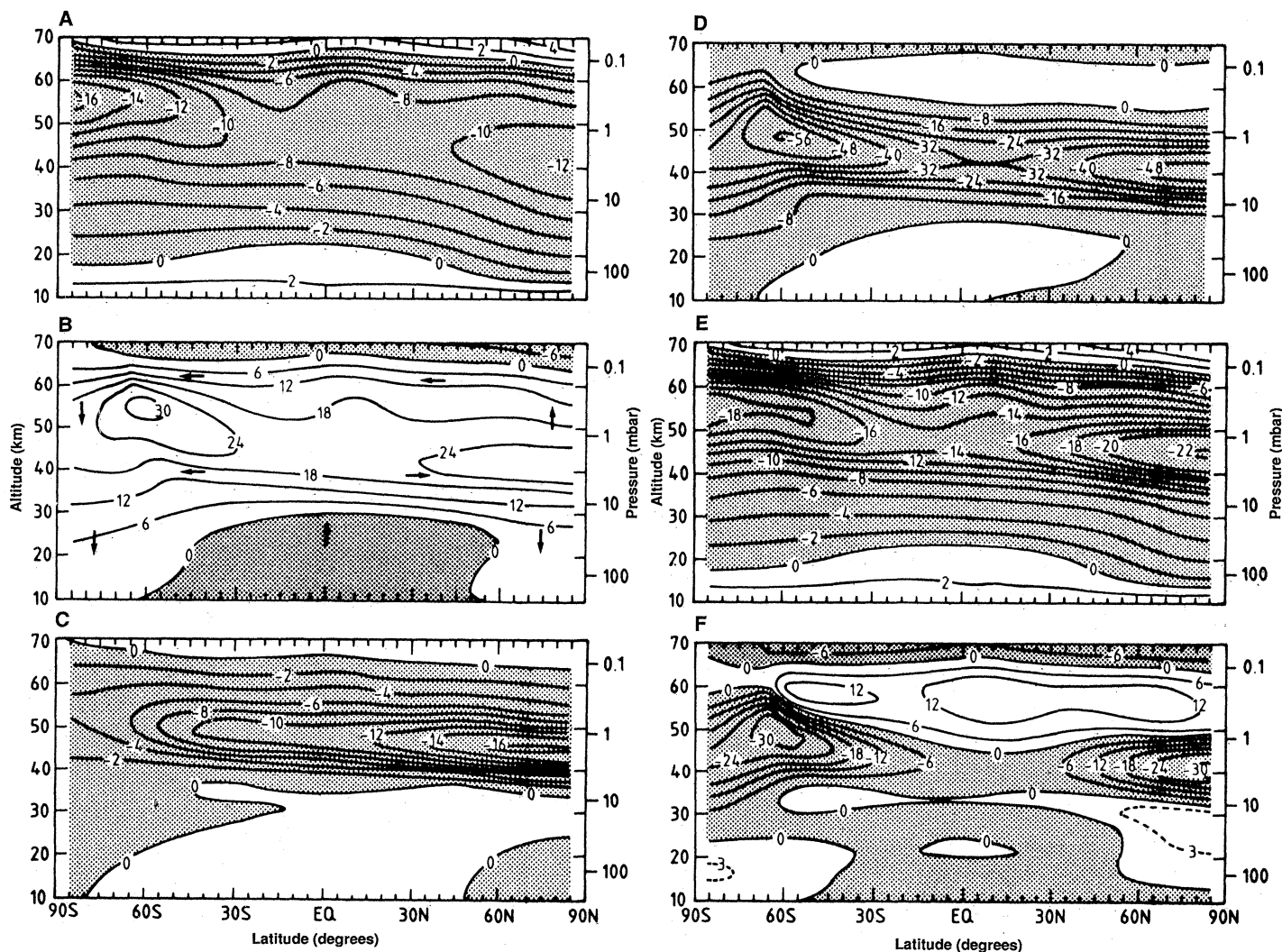


Fig. 1. (A and B) Response of the middle atmosphere in June to a doubling of CO₂. The calculated changes in temperature [(A), contour interval 2 K], are positive in the troposphere and lower stratosphere because of the greenhouse effect. They are negative throughout most of the stratosphere and lower mesosphere, with the strongest cooling in the vicinity of the stratopause. Ozone changes [(B) contour interval 6%] are largely anticorrelated with temperature changes as a result of the temperature dependence of reactions governing ozone concentration. Ozone values should also increase in the polar lower stratosphere due to poleward and downward transport. Schematic arrows indicate zonal mean air motions. (C and D) Middle atmosphere response due to a change in chlorofluorocarbons corresponding to an increase in odd chlorine from 2.0 to 6.6 ppbv. The largest ozone depletion (D) is found between 40 and 50 km at higher latitudes. Because of

the strong downward motion over the southern winter pole, significant ozone depletions are expected down to the tropopause. Maximum cooling (C) occurs just above the level of maximum ozone depletion because of reduced insolation absorption by ozone. The contour interval for ozone change is 8%. (E and F) Middle atmosphere response due to combining the above perturbations of CO₂ and odd chlorine, and simultaneously doubling the amount of CH₄ and increasing N₂O by 20%. Significant ozone depletions produced by the CFCs appear in the upper stratosphere at high latitudes, but the magnitude of this change is reduced compared with (C) and (D) by the effect of the CO₂ increase. Increases in CO₂ are responsible for the ozone increases of 5 to 10% in the lower mesosphere and of 2 to 5% in the polar lower stratosphere.

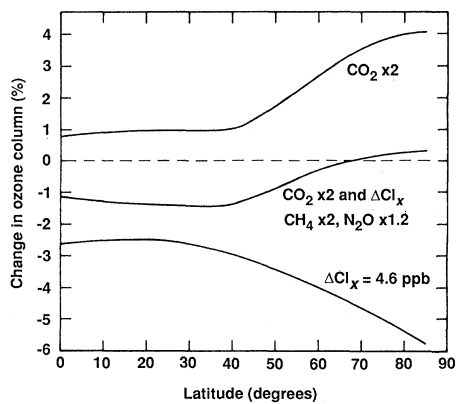


Fig. 2. Percent change in the ozone column as a function of latitude due to a doubling of carbon dioxide (Fig. 1, A and B), an increase in the amount of odd chlorine from 2.0 to 6.6 ppbv (Fig. 1, C and D), and from combining these two perturbations with a doubling of CH_4 and an increase in the amount of N_2O by 20% (middle curve, Fig. 1, E and F). Values plotted are averages of summer and winter hemispheric values.

In the polar lower stratosphere and upper troposphere, ozone increases of 3 to 6% are predicted. As the arrows in Fig. 1B indicate, in the mesosphere, air is transported toward the winter pole and downward. In the stratosphere, air is transported toward both poles and downward. Thus air enhanced in ozone is brought to the polar tropopause region. This circulation causes column ozone changes to be larger over the poles. Ozone increases in the lower stratosphere of ~20% are predicted by (6). Their colder temperatures and larger ozone increases reflect differences between radiative schemes, particularly the assumption of radiative equilibrium (6). The latitudinal variation in ozone changes near 20 km is somewhat sensitive to the meridional mixing associated with waves and to the boundary condition applied at 15 km for the residual mean circulation. Our mixing coefficients are comparable to those calculated from observations and 3-D calculations (10). The tropospheric forcing on the residual circulation, which is tuned to provide lower stratospheric temperatures in agreement with observations, is kept unchanged for the perturbation cases.

As shown by earlier 2-D model studies (3, 4), increased CFCs cause ozone depletion, with losses of 40 to 50% near the stratosphere (Fig. 1D). Significant ozone reductions occur below 30 km at high latitudes because of the transport of ozone-depleted air down over the winter pole (4). In the model this circulation is driven primarily by gravity wave absorption in the upper stratosphere and mesosphere and by Rossby wave absorption in the stratosphere, factors that can change when the temperature and zonal

wind change. Again, at lower latitudes below 25 km, ozone changes are predicted to be opposite to those in the rest of the stratosphere because of the self-healing effect. With less ozone there will be less UV absorption and the temperature will decrease. Temperature decreases are expected to be largest just above the level of maximum ozone decreases (Fig. 1C). Little change is expected in middle and lower stratospheric temperatures from CFC increases.

In order to study the response of the atmosphere to simultaneous disturbances of different origin and to simulate a possible state of the atmosphere corresponding to the middle or end of the next century, methane was doubled from 1.7 ppmv and nitrous oxide (N_2O) was increased by 20% from 300 ppbv, in addition to the doubled CO_2 and increase in Cl_x from 2.0 to 6.6 ppbv. Methane is expected to enhance ozone density in the troposphere and lower stratosphere as a result of its oxidation chain and in the upper stratosphere by sequestering Cl as HCl (1). In the mesosphere, increased methane should lead to more OH, hence ozone destruction. Increased N_2O should lead to catalytic ozone destruction by NO_x species in the stratosphere.

The temperature changes due to these combined effects are large (Fig. 1E). The effects of increased CO_2 cooling and reduced O_3 heating are additive, but not linearly so. For example, at 50 km over the equator, temperature changes in Fig. 1, A, C, and E, are -9 K, -11 K, and -15 K, respectively. In the lower stratosphere the effect of CO_2 clearly dominates.

Changes in ozone levels from the combined effects are more complex. In the upper stratosphere, CFC-induced depletion appears to dominate, but with typical losses reduced to ~20% by the CO_2 effect. CO_2 -induced increases of 5 to 10% are found in the lower mesosphere and of ~3% in the polar lower stratosphere. Since ozone concentrations are largest in the lower stratosphere, these modest percent increases greatly influence the ozone column.

Ozone column changes are shown in Fig. 2 for each of the three model runs. Increased Cl_x alone causes a net ozone depletion that varies from 2.6% at the equator to 5.5% at the pole (average of summer and winter values). The corresponding losses for a case in which the Cl_x concentration is 11.6 instead of 6.6 ppbv are 6.0 and 16.1%, respectively. The ratio of depletion at high to that at low latitudes for CFC-only perturbations is 2 to 3, increasing with the magnitude of chlorine injection. A doubling of CO_2 alone leads to column ozone enhancement, increasing from 0.7% at the equator to 4.1%

at the pole. In both cases the largest column ozone changes occur at the poles, because much of the air in the polar lower stratosphere was at one time in the upper stratosphere, where photochemical ozone changes are larger.

For the particular combined scenario of run 3, ozone column losses of ~1% are predicted equatorward of 45° (containing 70% of the earth's surface area), and an ozone increase of 0.2% is predicted near the pole. The latitudinal variation of predicted changes in UV radiation reaching the earth's surface is significantly smaller in the combined scenario than when CFCs are considered alone. The curve for run 3 in Fig. 2 is probably within the error associated with model calculations, although this error is difficult to estimate. If a 9.6-ppbv increase is adopted for CFCs in the combined scenario, column ozone is expected to decrease by 3.7% at the equator and 8.1% at the poles.

The model suggests noticeable dynamical responses to these perturbations. As a result of temperature changes due to perturbations in radiatively active species, the distribution of zonal wind changes so that the propagation of gravity and Rossby waves is modified. For example, in run 3 changes of up to 15 m/sec occur in zonal wind and lead to changes in the vertical eddy diffusivity that reach 90% in the upper stratosphere (not shown). The feedback of wave mean flow dynamics on column ozone changes is, however, a secondary modification (11).

These model simulations confirmed that the sensitivity of the ozone column to increasing Cl_x is a factor of 2 to 3 times larger at high latitudes than in the tropics (3, 4), and also confirmed that the positive ozone changes resulting from increased CO_2 are significantly larger at the pole than at the equator (5, 6). Perturbations by CO_2 thus tend to reduce the latitudinal gradient in the column ozone depletion produced by the release of CFCs. The magnitude of the change in column ozone abundance is largely dependent on changes in the lower stratosphere, a region difficult to model because of the long radiative and chemical lifetimes involved and the delicate balance between radiative, dynamical, and chemical processes. In our model, transport is important in determining the latitudinal variation in column ozone changes.

REFERENCES AND NOTES

1. R. J. Cicerone, *Science* **237**, 35 (1987); R. E. Dickinson and R. J. Cicerone, *Nature (London)* **319**, 109 (1986).
2. L. B. Callis and M. Natarajan, *Geophys. Res. Lett.* **8**, 587 (1981); D. J. Wuebbles, F. M. Luther, J. E. Penner, *J. Geophys. Res.* **88**, 1444 (1983); G. Brasseur and A. De Rudder, *ibid.* **92**, 10903 (1987).
3. J. A. Pyle, *Pure Appl. Geophys.* **118**, 355 (1980); J.

- D. Haigh and J. A. Pyle, *Q. J. R. Meteorol. Soc.* **108**, 551 (1982); F. Stordal and I. S. A. Isaksen, *Tellus* **39B**, 333 (1987); H. S. Johnston *et al.*, *Atmospheric Ozone 1985* (World Meteorological Organization, Geneva, 1986), chap. 13.
4. S. Solomon *et al.*, *J. Geophys. Res.* **90**, 12981 (1985).
 5. J. D. Haigh, *Q. J. R. Meteorol. Soc.* **110**, 167 (1984).
 6. R. S. Eckman, J. D. Haigh, J. A. Pyle, *Nature (London)* **329**, 616 (1987). This study is based on a classical Eulerian 2-D model that includes most of the important feedbacks between chemistry and radiation but uses satellite data to specify momentum and heat fluxes associated with large-scale waves.
 7. J. J. Barnett, J. T. Houghton, J. A. Pyle, *Q. J. R. Meteorol. Soc.* **101**, 245 (1975); G. M. Keating, G. P. Brasseur, J. Y. Nicholson III, A. De Rudder, *Geophys. Res. Lett.* **12**, 449 (1985).
 8. H. J. Edmon Jr., B. J. Hoskins, M. E. McIntyre, *J. Atmos. Sci.* **37**, 2600 (1980); T. J. Dunkerton, C. P. F. Hsu, M. E. McIntyre, *ibid.* **38**, 819 (1981).
 9. R. S. Lindzen, *J. Geophys. Res.* **86**, 9707 (1981); G. Brasseur and M. Hitchman, in *Proceedings of the NATO Workshop on Middle Atmosphere Transport* (Reidel, Dordrecht, 1987).
 10. M. H. Hitchman and G. Brasseur, unpublished results. Mixing and the meridional circulation caused by Rossby waves are parameterized in the 2-D model by using the conservation of wave activity principle. Rossby wave activity is produced in a climatological fashion at the tropopause, advected by a group velocity that evolves with the model zonal winds, and is damped at upper levels. Absorption of Rossby wave activity causes both an easterly torque and irreversible mixing. This parameterization provides a self-consistent coupling of the wave activity with the winds, tracer distributions, and the radiative field.
 11. D. L. Williamson, J. T. Kiehl, V. Ramanathan, R. E. Dickinson, J. J. Hack, *NCAR Tech. Note 285* (National Center for Atmosphere Research, Boulder, CO, 1987).
 12. G. Brasseur and S. Solomon, *Aeronomy of the Middle Atmosphere* (Reidel, Dordrecht, 1987).
 13. W. B. De More *et al.*, *JPL Publ. 85-97* (National Aeronautics and Space Administration/Jet Propulsion Laboratory, Washington, DC, 1985); G. Brasseur and P. C. Simon, *J. Geophys. Res.* **86**, 7343 (1981).
 14. M. C. McCracken and F. M. Luther, *U.S. Dep. Energy DOE/ER-0237* (1985).
 15. C. B. Leovy, in *Dynamics of the Middle Atmosphere* (Terra Scientific, Tokyo, 1984).
 16. The National Center for Atmospheric Research is sponsored by the National Science Foundation. We thank J. T. Kiehl for providing the radiative code and J. C. Gille and B. A. Boville for useful discussions.

6 November 1987; accepted 19 February 1988

Iron Photoreduction and Oxidation in an Acidic Mountain Stream

D. M. MCKNIGHT, B. A. KIMBALL, K. E. BENCALA

In a small mountain stream in Colorado that receives acidic mine drainage, photoreduction of ferric iron results in a well-defined increase in dissolved ferrous iron during the day. To quantify this process, an instream injection of a conservative tracer was used to measure discharge at the time that each sample was collected. Daytime production of ferrous iron by photoreduction was almost four times as great as nighttime oxidation of ferrous iron. The photoreduction process probably involves dissolved or colloidal ferric iron species and limited interaction with organic species because concentrations of organic carbon are low in this stream.

HYDROUS IRON OXIDES, WHICH commonly occur in aquatic environments, may influence the chemistry and transport of trace metals and natural organic material by adsorption and coprecipitation reactions. We present results of a field experiment in which production of ferrous iron, Fe(II), by photoreduction was measured quantitatively in a small Rocky Mountain stream that receives acidic mine drainage. A well-defined increase in dissolved Fe(II) occurred with increasing light intensity. There are several pathways by which diel cycling of iron through photoreduction and oxidation will influence other chemical or microbial processes. This diel cycle may contribute to the increased abun-

dance of amorphous iron oxides over that of more crystalline forms in streams; amorphous oxides are more reactive in adsorbing metal and organic species (1). Diel photoreduction and oxidation of iron, and other metals such as copper (2), may be a source of scatter in long-term data sets of metal concentrations in acidic streams and lakes (3).

St. Kevin Gulch, in Colorado, is representative of the more than 600 km of stream reach in the state that is contaminated with acidic mine drainage (4). This small tributary of Tennessee Creek is located 7 km northwest of Leadville and receives acidic, metal-enriched drainage (5) from mine tailings and abandoned mines (Fig. 1). Silver sulfide ore in veins in quartz-biotite-feldspar schist and gneiss was mined more than 80 years ago. The 247-m reach that was studied (between sites SK40 and SK50 in Fig. 1) begins 1185 m downstream from the in-

flows from the tailings. Hydrous iron oxides are abundant on the stream bed in the study area.

Accurate measurement of discharge is necessary for calculation of mass flow (6). We used the dilution gauging technique (7, 8); a solution of 4.8M LiCl was injected into the stream at a site 360 m above the mine at a constant rate of 27 ml min⁻¹ during a 36-hour period. The steady-state Li⁺ concentration was 0.76 ± 0.02 mg liter⁻¹ at SK40 and 0.75 ± 0.02 mg liter⁻¹ at SK50 (mean ± SEM, n = 40). Background Li⁺ concentrations were approximately 0.004 mg liter⁻¹. Discharge was calculated from the mass balance of the injected Li⁺ and the concentration of Li⁺ in the stream for each time point at both sites. The travel time was about 4 hours from the mine site to SK40 and was 40 minutes from SK40 to SK50, as determined by comparing the leading and trailing edges of the injected tracers (7, 8).

Samples were collected at hourly intervals at SK40 and SK50 from before sunrise at 0500 on 19 August 1986 until 1800 on 20 August 1986 (9, 10). The iron concentrations that were determined by inductively coupled plasma spectrophotometry (ICP) for the 0.1-μm filtered samples (filterable iron) were consistently greater than iron concentrations that were obtained with addition of the hydroxylamine reductant in the colorimetric procedure (reactive iron) (Table 1). Ultrafiltration measurements showed that colloidal iron was about 50% of the filterable iron; because this amount was more than the difference between filterable and reactive iron, reactive iron probably included some colloidal iron as well. We calculated the activity ratio Fe²⁺/Fe³⁺ and thus Eh by estimating ferric iron, Fe(III), as the difference between reactive and ferrous iron as determined colorimetrically; the program WATEQF (11) was used to calculate iron speciation (12).

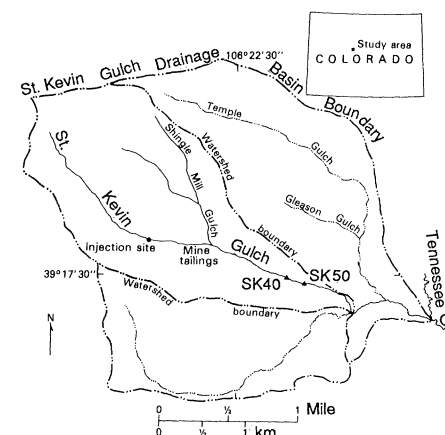


Fig. 1. Map of St. Kevin Gulch. The catchment area at SK50 is 3.9 km².

D. M. McKnight and B. A. Kimball, U.S. Geological Survey, Water Resources Division, Denver Federal Center, Denver, CO 80225.
K. E. Bencala, U.S. Geological Survey, Water Resources Division, 345 Middlefield Road, Menlo Park, CA 94025.